Radiation pattern and seismic waves generated by a working roller-cone drill bit

James W. Rector III* and Bob A. Hardage‡

ABSTRACT

The seismic body wave radiation pattern of a working roller-cone drill bit can be characterized by theoretical modeling and field data examples. Our model of drill-bit signal generation is a pseudo-random series of bit-tooth impacts that create both axial forces and tangential torques about the borehole axis. Each drill tooth impact creates an extensional wave that travels up the drill string and body waves that radiate into the earth. The model predicts that P-waves radiate primarily along the axis of the borehole, and shear waves radiate primarily perpendicular to the borehole axis. In a vertical hole, the largest P-waves will be recorded directly above and below the drill bit; whereas, the largest shear waves will be recorded in a horizontal plane containing the drill bit. In a deviated borehole, the radiation patterns should be rotated by the inclination angle of the drill bit. This proposed seismic body wave radiation pattern is investigated with field data examples.

The presence of the drill string in the borehole creates other wave modes that are not typically observed when conventional vertical seismic profiles (VSPs) are conducted in fluid-filled wells. For example, the extensional wave traveling up the drill string creates a head wave traveling away from the drill string, provided the formation velocities adjacent to the borehole are less than the drill-string velocity. Likewise, when the extensional wave traveling up the drill string reaches the drill rig, some of the energy continues through the drill rig structure, re-enters the earth, and travels away from the rig as ground roll or shallow refractions. Secondary events are radiated at the drill bit after they travel up the drill string, reflect off drill-string discontinuities, and travel back down the drill string to the bit. Each of these drill-bit arrivals has a characteristic moveout as a function of wellhead offset and drill-bit depth. A knowledge of the radiation patterns and the wave modes generated by the drill bit is essential to interpreting drill-bit wavefields.

INTRODUCTION

The drill-bit VSP technique uses, as a downhole seismic energy source, the vibrations produced as the drill bit impacts the formation during drilling. The drill-bit signals are recorded at the surface using an accelerometer attached to the top of the drill string and conventional seismic sensors such as geophones or hydrophones at selected offset locations. The vertical accelerometer recording is used as a pilot signal—analogous to the vibroseis sweep signal—and is crosscorrelated with the geophone recordings. Deconvolution and time shifts (Rector and Marion, 1991) are used to compensate the crosscorrelated data for the location of the pilot sensor, which is distant from the drill-bit energy source.

A rotary roller-cone bit is designed to break rock through shear and compressive failure (Adams, 1986). As shown in Figure 1, the principal force applied to the formation by this type of bit is directed axially (vector F_V). A smaller force component is directed horizontally (vector F_H). In contrast to roller-cone drill bits, polycompact bits and diamond bits break rock through a shearing or grinding action (Vennin, 1989). In unpublished reports, this type of drill-bit action has been observed to create lower drill-bit signal levels. The chiseling action of the drill-bit teeth into the formation launches extensional waves traveling along the drill string (Squire and Whitehouse, 1979) at a velocity that appears to be slightly lower than the longitudinal wave velocity of a steel rod (Rector and Marion, 1991), and also radiates

seismic body waves into the earth. Our model of the body wave radiation pattern assumes that the drill-bit arrivals obtained in the crosscorrelated data originate as impacts of the drill-bit teeth against the formation. Using an axial impact model for the roller-cone drill-bit source orientation, we examine the body wave radiation pattern with a theoretical model and real data examples.

When recording conventional VSP and acoustic logs, the presence of the borehole creates guided waves, such as Stoneley waves, that travel up and down the fluid column and the formation interface. The main differences in the characteristics of conventional VSP wave propagation in the borehole and a drill-bit-generated wavefield is due to the presence of the drill string attached to the drill-bit source. The partial replacement of borehole fluid with a steel drill string has an effect on the boundary conditions of the borehole system, modifying wave propagation inside the borehole and in the earth outside the borehole. We draw upon theoretical models of wave propagation and real data examples to characterize the borehole wave types generated when a drill string occupies the borehole.

Conventional VSP data processing and analysis use the time moveout over receiver depth and source offset as a means to distinguish and filter different wave modes (Hardage, 1985). Direct and reflected P-waves can be distinguished from shear waves and Stoneley waves by identifying the relative moveouts of each wave mode. This type of analysis can also be used with drill-bit data. However, the presence of the drill string and the use of a pilot sensor at the top of the drill string change the moveout characteristics of the wave modes. In this paper, we describe the moveout characteristics of the different drill-bit modes and present methods for attenuating undesired modes.

RADIATION PATTERN OF A ROLLER-CONE DRILL BIT

We separate the characterization of drill-bit radiation into an analysis of the radiation distribution produced by axial forces and the radiation distribution produced by transverse forces.

Radiation from the axial forces produced by a roller-cone bit

The seismic radiation pattern proceeding from the axial component drill-bit impacts can be modeled as a transient, monopolar point force acting along the axis of the borehole (White, 1965). White (1965) and Heelan (1953) showed that the far-field radial displacement resulting from a point force, $g(t)$, applied along the axis of a cylinder embedded in an isotropic, homogeneous solid is:

$$U_r(r, \phi, t) = \frac{A_1 \cos \phi}{\rho \alpha^2 r} g\left(t - \frac{r}{\alpha}\right), \qquad (1)$$

and the far-field angular displacement is:

$$U_\phi(r, \phi, t) = \frac{A_1 \sin \phi}{\rho \beta^2 r} g\left(t - \frac{r}{\beta}\right), \qquad (2)$$

where ρ is the formation density, r is the straight line distance from the source to the wavefront, α and β are the formation compressional and shear velocities, A_1 is a scalar, and the angle ϕ is measured relative to the direction of the point force (i.e., relative to the direction of axial drill-tooth impacts at the bottom of the borehole). U_r represents P-wave radiation since it is a component of motion that is oriented radially away from the source. U_ϕ represents SV-wave motion since its particle displacement is in a plane containing the cylinder axis and perpendicular to U_r. There are no SH-waves radiated by this pure axial impact. The P and SV radiation patterns have rotational symmetry about the cylinder axis, and when the wavelengths of the body waves are much greater than the borehole radius, the far-field displacements are not influenced by the presence of the borehole.
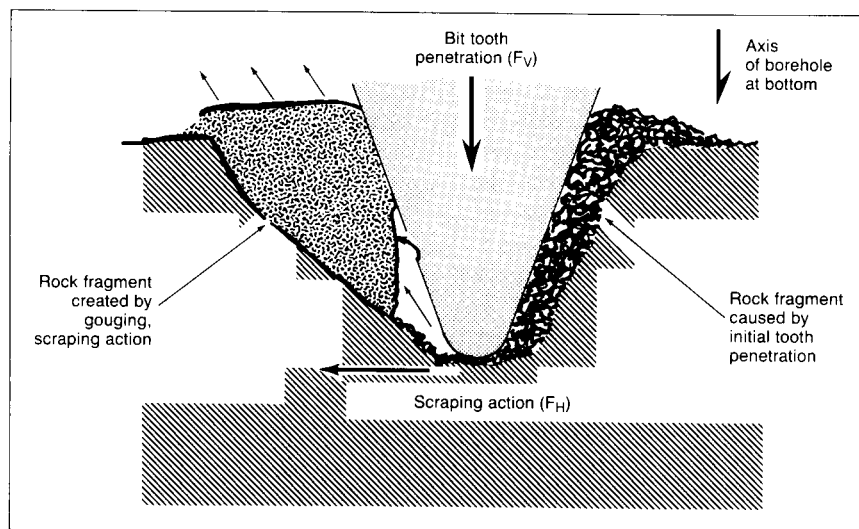

FIG. 1. Action of a roller-cone drill bit at the bottom of a borehole [taken from Adams, (1986)].

The calculated P-wave and SV-wave displacements corresponding to equations (1) and (2) are shown in Figure 2. P-waves are radiated along the direction of the axial tooth impact, with no P-wave energy radiated perpendicular to the force direction. SV-waves are radiated perpendicular to the impact axis, and no SV-waves are radiated along the axis. The relative amplitudes of the P- and SV-radiation lobes are determined by the Poisson's ratio of the formation being impacted by the drill bit. If the formation has a Poisson's ratio of 0.25, the SV-wave displacement at an angle of 45 degrees from the impact axis will be three times larger than the P-wave displacement, and the displacements will be equal when $\phi = 18$ degrees.

Radiation from the transverse forces generated by a roller-cone bit

One laboratory measurement of the transverse forces created by a tri-cone bit is summarized in Sheppard and Lesage (1988). This laboratory experiment indicated that transverse drill-bit impacts occur in synchronization with axial impacts. Thus, a roller-cone bit produces the same number of transverse impulses as it does axial impulses. However, the magnitude of the transverse forces are significantly less than the magnitudes of the axial forces. A conclusion that can be made is that a roller-cone bit will generate some SH signal because of this transverse action. The lab experiment also indicated that the transverse impacts create a sequence of force couples at the bottom of the borehole during each rotation of a roller cone.

The lab measurements do not represent realistic drilling conditions in the sense that the lab weight-on-bit (WOB) forces are quite low. These forces have to be scaled up by a factor of 10 to 30 to represent normal drilling WOB values of 20 000 to 50 000 lbs (9060 to 22 650 kg). A question to ask is whether these laboratory measurements still apply at higher force regimes. We will assume that these low-force-level lab tests do adequately describe how drill-bit forces are created and how they are oriented. Also the lab measurements were made under atmospheric conditions. Again, we will assume that these lab-observed force relationships are in effect when the bit teeth cut rock at the bottom of a deep well having a large hydrostatic head.

The particle displacement created by a pair of symmetrically distributed force couples has been solved in the literature (White, 1965). The particle displacements produced by two force couples acting in a horizontal plane within a well are described by the functions:

$$U_\theta = -\frac{A_2 d \sin \phi}{4\pi\rho\beta^3 r} g'\left(t - \frac{r}{\beta}\right) \qquad (3)$$

$$U_r = 0$$

$$U_\phi = 0,$$

where g' is the time derivative of the impulse function produced by the couple, r is the radial distance to the point where the displacement is measured, d is the distance between the two force vectors comprising the couple, A_2 is a scalar, ρ is formation density, β is formation shear velocity, θ is the azimuth angle measured in the xy-plane, and ϕ is the angle between the z-axis and the radial vector.

An unscaled representation of the calculated SH radiation pattern associated with this displacement behavior is shown in Figure 2. The SH signal is the smallest contributor to the total particle displacement since the SH amplitude is produced by a transverse force couple having a smaller amplitude than the vertical force that produces the P and SV displacements, and in addition, the SH amplitude is scaled by a factor proportional to (fd/β^3), where f is the frequency in Hz, rather than by $(1/\alpha^2)$ or by $(1/\beta^2)$ as are the P and SV amplitudes. For typical drill-bit diameters and seismic frequencies, the SH displacement will be approximately three orders of magnitude lower than the SV displacement.

FIELD DATA INVESTIGATIONS OF THE ROLLER-CONE DRILL-BIT RADIATION PATTERN

The radiation pattern shown in Figure 2 predicts that in a vertical well drilled in an isotropic, horizontally layered earth, geophones deployed on the earth's surface directly above the drill bit will receive only P-waves from the drill bit. At positions offset from the borehole, the SV and SH radiation lobes begin contributing to the response at the surface.

Vertical geophone characterization of drill-bit P-wave radiation

Figure 3a shows drill-bit data that were recorded with a series of vertical geophone arrays extending away from the wellhead. Geophone arrays were deployed at 100 ft (30.5 m) intervals on the surface beginning at a distance of 1300 ft (396 m) from the wellhead and ending 4600 ft (1402 m) from the wellhead. Each array consisted of four 4.5 Hz geophones placed 25 ft (7.6 m) apart. The crosscorrelated traces were computed over a recording time of 10 minutes as a vertical well was drilled with a roller-cone bit at a depth of 3290 ft
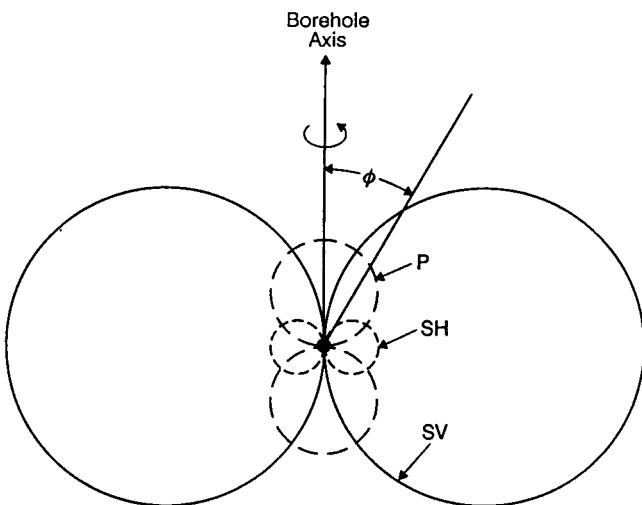

FIG. 2. Far-field body wave amplitude distributions produced by a roller-cone bit-tooth impact at the bottom of the borehole. The relative amplitude of the P-wave radiation lobe to the SV-wave radiation lobe is drawn for a formation with a Poisson's ratio of 0.25. The SH lobe is about four orders of magnitude less than shown.

(1003 m). The traces in Figure 3a are displayed with a fixed gain so that the relative amplitudes between traces can be estimated. The *P*-wave direct arrival is identified by its hyperbolic moveout with offset and its correlation time. The other hyperbolic moveout events are drill string multiples, and the linear moveout event that crosses the direct arrival is a rig arrival (these arrivals are discussed in a later section). The amplitude of the direct arrival is greater at the near offsets and decreases uniformly as the offset distance and the takeoff angle φ increase. This behavior qualitatively agrees

with the amplitude response of the upward traveling *P*-wave radiation depicted in Figure 2.

To use the direct-arrival amplitudes for estimating the *P*-wave radiation pattern, the data at offset distance *x* can be corrected for spherical spreading, absorption, and for the vector response of the vertical geophone. Figure 3b compares the magnitude of the theoretical drill-bit *P*-wave radiation [obtained from equation (1)] with the measured *P*-wave radiation as a function of φ. The measured radiation was obtained by computing the *P*-wave direct-arrival peak amplitude for each trace and correcting for spreading, absorption, and the receiver vector response (assuming $f = 30$ Hz, $Q = 50$, and a constant velocity of 8000 ft/s (2430 m/s), which are reasonable values for the region). The measured values were then scaled to the median amplitude computed from the first five offsets. The computed amplitudes exhibit a great deal of scatter, but the general trend with offset is similar to the theoretical curve. The high-frequency data scatter is probably due to receiver coupling variations and to overlapping rig and head wave arrivals (discussed in a later section).

Three-component geophone characterization of drill-bit radiation

Figure 4 is a three-component, roller-cone bit wavefield recorded at an offset of 3500 ft (1067 m) from a vertical well.
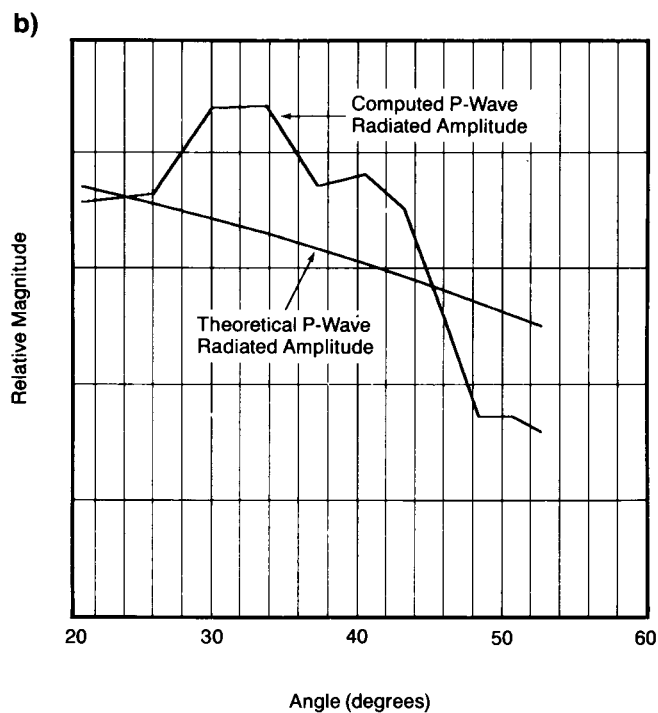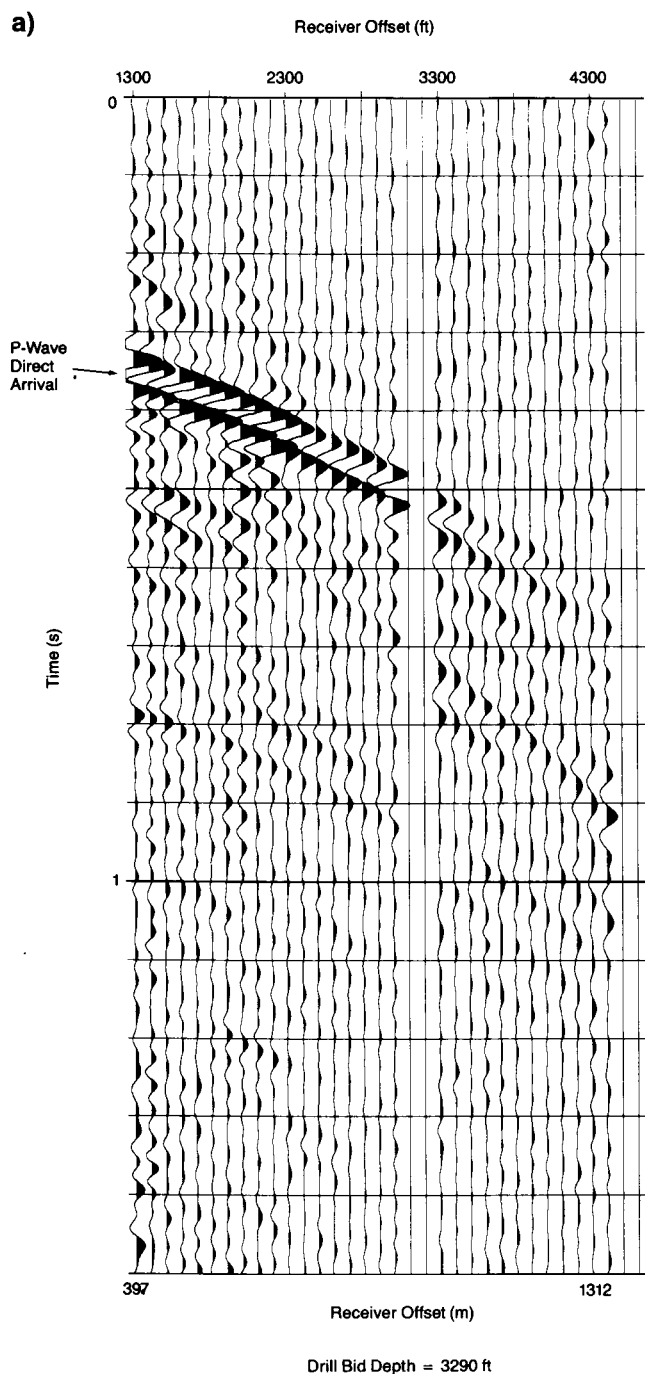

FIG. 3. (a) Wavefield recorded when the drill bit was drilling in a vertical well at a depth of 3290 ft (1003 m). Each trace represents the crosscorrelation function between the pilot signal recorded at the top of the drill string and a different geophone array on the earth's surface. The *P*-wave direct-arrival amplitude decreases with increasing offset from the wellhead. (b) Measured versus theoretical *P*-wave radiation as a function of angle φ. The measured values were taken from the data in Figure 3a after correcting for attenuation and receiver response.

The vertical component was recorded with an array of twenty-four 10 Hz vertical geophones distributed over 250 ft (76.9 m). The two horizontal components were oriented transversely and radially in line to the wellhead and were recorded by two in-line arrays of 12 Hz horizontal geophones spanning 100 ft (30.5 m).

The compressional and shear direct arrivals labeled in Figure 4 are identified based on their traveltimes and moveouts. The display in Figure 4 was scaled by normalizing each trace to its peak rms amplitude. Hence, the relative amplitudes of the arrivals cannot be estimated. However, the improvement in the P-wave direct-arrival S/N and the degradation of shear direct with depth (i.e., with decreasing angle ϕ) are in qualitative agreement with equations (1) and (2). The radial component records shear direct arrivals with higher S/N than the transverse component, indicating that the radiated shear SV energy from the drill bit is greater than the SH energy, as proposed by Figure 2.

Figure 5a shows a three-component trace from a depth of 4440 ft (1353 m) that is recorded at a receiver offset of 3500 ft (1066 m) and displayed in true relative amplitude. The P-wave direct arrival on the vertical component has an amplitude that is approximately equivalent to the shear-wave direct arrival on the radial component. By contrast, equations (1) and (2) would predict a shear-wave direct arrival about three times the P-wave direct arrival amplitude. Assuming these arrivals traverse similar earth paths, the discrepancies between observation and theory could be due to coupling differences between the geophones or differences in compressional and shear Q.

A quantitative estimate of the drill-bit radiation pattern can be obtained from the measured direct arrival amplitudes in several ways. Like the analysis with offset, the direct arrival amplitudes can be scaled for attenuation and receiver vector response and then compared with curves defined by equations (1) and (2). However, this method assumes that the drill-bit source amplitude is constant. Scatter in the measurements can be introduced by impedance changes over depth, coupling changes, and changes in drilling parameters.

A robust estimate of the drill-bit radiation is to analyze the variation in the *ratio* of shear to P-wave direct-arrival amplitude with depth. At a given drill-bit depth, the body waves have the same source amplitude and similar raypaths, so there is no need to apply a depth-dependent scaling factor to the data. Figure 5b shows a comparison of this measured ratio and a theoretical curve. The theoretical curve was adjusted to incorporate the differences between the measured and the theoretical amplitude ratios observed in Figure 5a. The ratios were measured at particular depths where the S/N of both arrivals was high. After adjustment, the theoretical and measured curves give generally good agreement.

OTHER WAVE MODES GENERATED BY THE DRILL BIT

Besides the primary body waves radiated into the earth at the drill bit, there are other mechanisms by which drill-bit vibrations are theoretically transferred into the earth and recorded by surface geophones. These other wave modes are caused by energy transfer between the wave traveling in
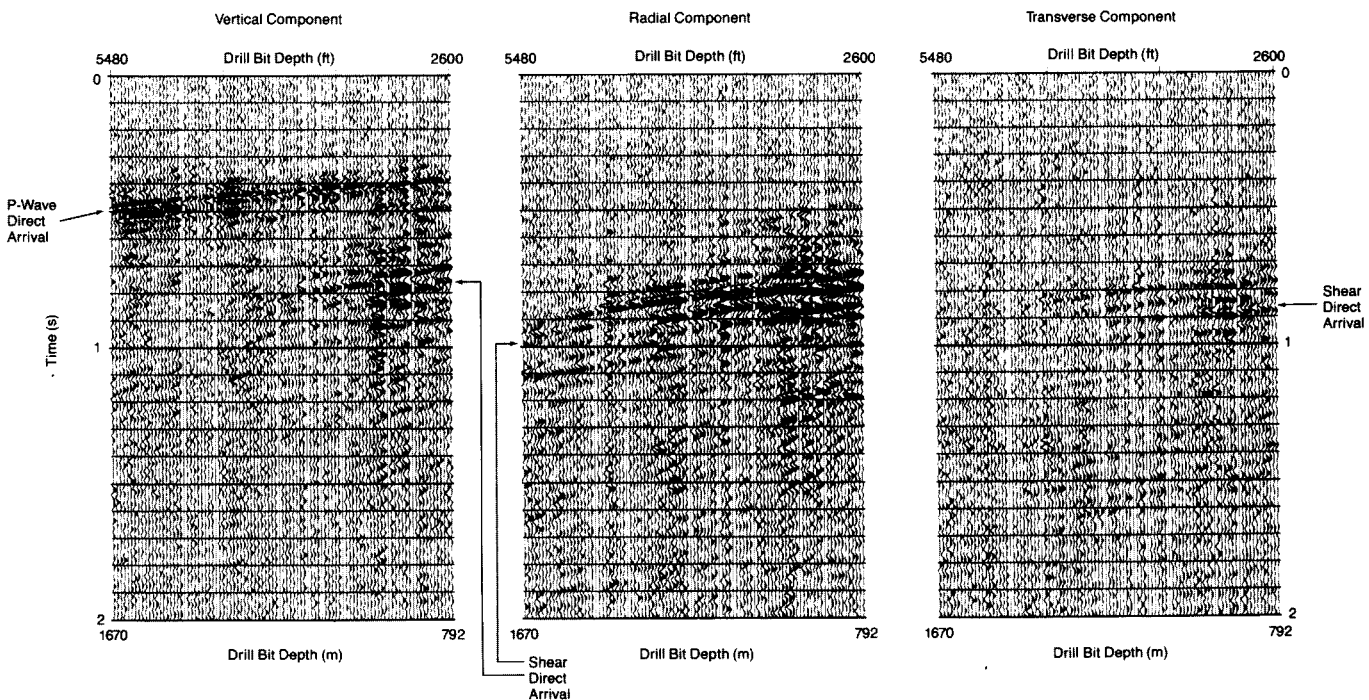

FIG. 4. Drill-bit wavefields recorded at a three-component geophone group located 3500 ft (1067 m) from the wellhead of a vertical well. The traces represent drilling depths from 2600 to 5480 ft (792 to 1670 m). The P-wave direct arrival from the drill bit to the geophone array, as well as a shear-wave direct arrival are labeled. The data are displayed after normalizing each trace to its maximum amplitude and thus correct amplitude changes from trace to trace cannot be observed.

a)

P-Direct
Arrival →
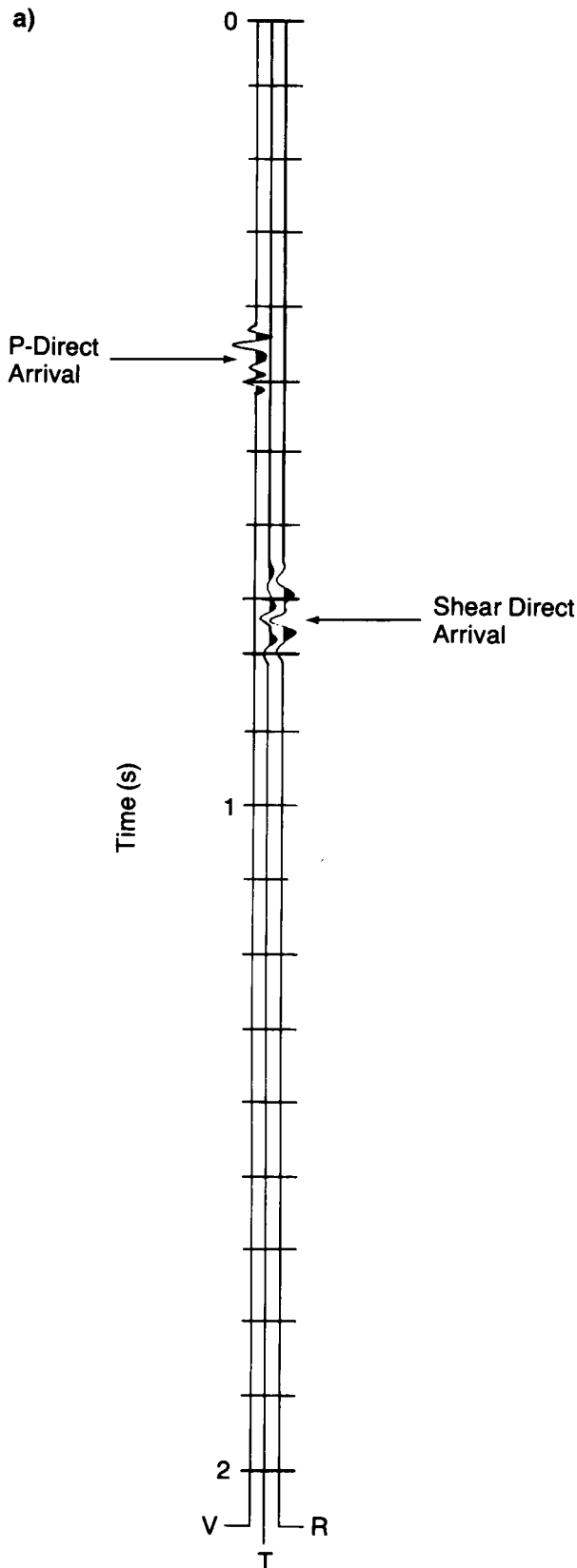
← Shear Direct
Arrival

Time (s)

0

1

2

V — L R
T

Fig. 5a. Three-component (Vertical (V), Radial (R), and Transverse (T)) response corresponding to the traces at a depth of 4440 ft (1354 m) in Figure 4, displayed in true relative amplitude.

the drill string and the formation. Before discussing correlated field examples we model a few of the principal travel paths taken by these other wave modes.

Rig generated arrivals

In correlated drill-bit wavefields recorded by surface geophones, one of the principal arrivals has a delay and a moveout with depth and offset that identify it as having a source location at the drill rig. As shown in Figure 6, this "rig-generated" arrival is modeled as traveling from the drill bit up the drill string, entering into the rig mast via the drilling lines, and traveling into the earth through the feet of the rig mast. A group of surface-geophone arrays extending away from the wellhead would be expected to record rig-generated arrivals similar to a "shot" gather in conventional surface seismic acquisition, with the shot positioned at the drill rig.

Head wave arrivals

Besides the drill rig, the drill string itself can act as a secondary radiator of drill-bit energy. When the velocity of the extensional wave traveling along the drill string is greater than the formation velocity, the extensional wave traveling in the drill string is transmitted into the earth away from the drill string, forming a wavefront with characteristics similar to head waves following along a high velocity layer. As drill-string extensional wave velocities are typically 15 600 ft/s (4758 m/s), head waves should be common in wells drilled in sedimentary rock. Head waves were predicted by White (1965) who described them in three dimensions as conical waves. In conventional VSP where the borehole does not contain a drill string, the propagation velocity in the borehole (i.e., the fluid velocity) is generally less than the formation velocities and no head waves are radiated into the far-field. In some unconsolidated sediments, the shear velocity can be less than the fluid velocity. In these instances, shear head waves, also called Mach waves (Meredith 1990) are produced.

As with energy partitioning in conventional tube wave analysis, the impedance mismatch between the drill string, the fluid, and the formation would be expected to produce a head wave displacement in the earth that is only a small fraction of the radial component of the extensional wave displacement in the drill string. However, unlike tube waves, whose amplitude decreases exponentially away from the borehole wall, the head wave is reinforced as it travels away from the borehole, and its amplitude theoretically decreases as the square root of the distance from the borehole (see Appendix). Thus, in theory, head waves can be recorded with geophone arrays on the surface a long distance from the wellhead. Finite-element modeling (Samec and Kostov, 1988) of an axial force at the bottom of a borehole containing steel drill string surrounded by drilling fluid has predicted these head waves, and from finite-element modeling, Samec (1989 Stanford University, personal communication) obtained head waves at the surface that were of comparable magnitudes to primary body waves from the drill bit. In the examples that follow, we will be discussing head waves that propagate into the earth as compressional waves, although shear head-wave modes radiating from the drill string also exist.

As shown in Figure 6, in the far-field of a homogeneous solid, the wavefront normal of the head wave makes an angle θ_c with respect to the borehole-axis normal where:

$$\theta_c = \sin^{-1} \frac{V_f}{V_{DS}} \quad (V_f < V_{DS}).\qquad(4)$$

In equation (4), V_f is the formation velocity and V_{DS} is the velocity of the drill string extensional wave. Near the borehole, the wavefront is defined by a modified Hankel function (see Appendix) and at the borehole, the head wave has a wavefront normal that parallels the drill-string axis. The raypaths taken by the head wave from the drill string to the earth's surface are depicted in Figure 6 for a formation velocity of 10 000 ft/s (3048 m/s). For a vertical borehole in a constant velocity earth, receivers placed at the surface near the rig record head waves that emanate from the drill string near the surface, while longer surface offsets record head waves that arrive from deeper portions of the drill string.

In most formations, the extensional wave traveling along the drill string propagates with a velocity that is higher than the formation velocities adjacent to the drill string. However in a few situations, i.e., hard limestones, anhydrites, evapor-

ites, and granite, the formation P-wave velocity can be higher than the extensional wave velocity. In this situation, the critical angle θ_c in equation (4) is undefined, and a compressional head wave is not predicted to exist (a shear head wave would still exist in these situations). Instead, a guided wave would theoretically be generated. As shown in the Appendix, this wave travels along the borehole at the velocity of the extensional wave in the drill string; however, like a tube wave, its amplitude decreases exponentially away from the borehole wall, and very little of its energy reaches the surface geophone arrays via direct paths through the earth. Like tube-wave arrivals in conventional VSP, transfer of the guided wave energy into the earth may result after mode conversion at borehole discontinuities.

Drill string multiple arrivals radiated at the drill bit

Besides the body waves radiated into the earth at the drill bit and the other wave modes radiated by the extensional wave traveling in the drill string, multiple energy is also radiated into the earth via all the mechanisms shown in Figure 6 after undergoing one or more reflections from discontinuities within the drill string. These multiple arrivals
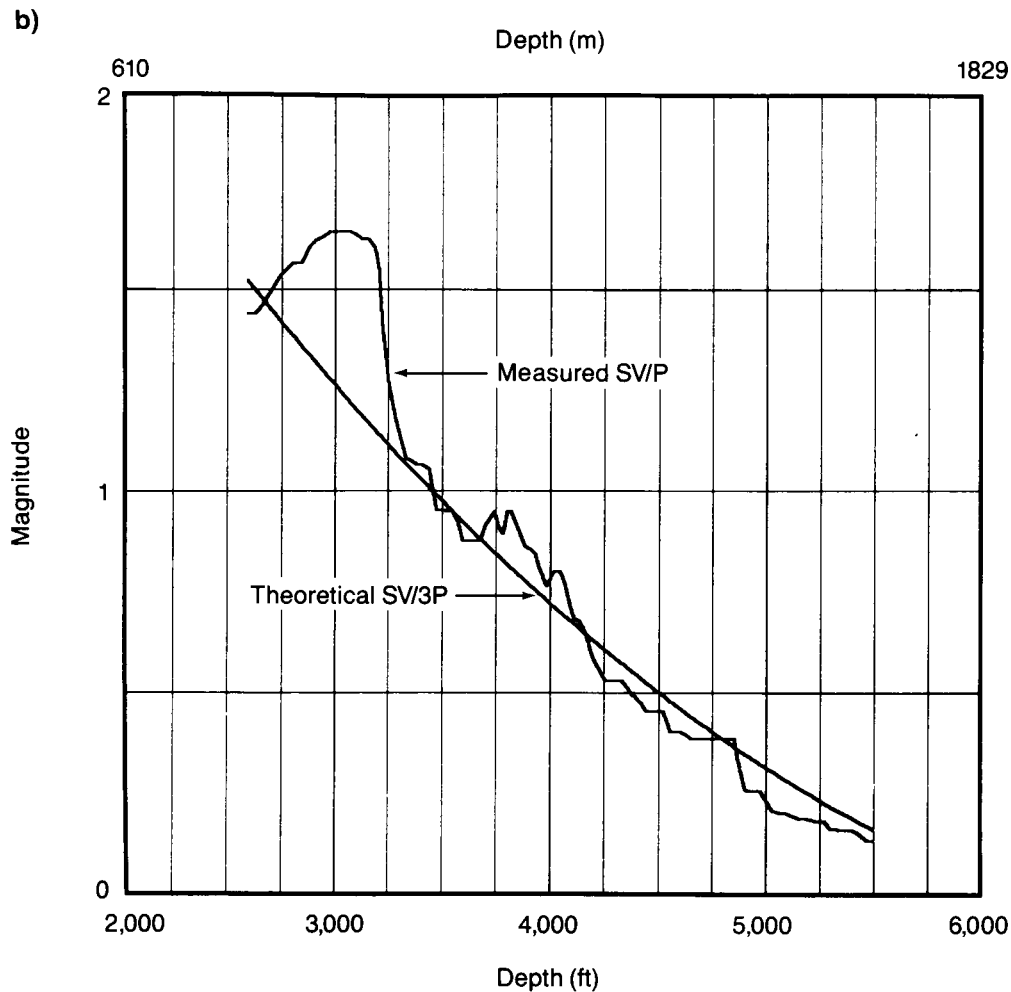

FIG. 5b. Measured versus theoretical SV to P-wave radiation as a function of depth. The theoretical curves were corrected for the higher absorption of the shear waves observed in Figure 5a. The factor of 3 in the denominator of the theoretical curve label results from assuming the formation velocities α and β in equations (1) and (2) can be approximated by $(\alpha^2/\beta^2) = 3$.

have been observed on the response of the pilot sensor recorded at the top of the drill string (Rector and Marion, 1991). A bottom hole assembly (BHA) multiple is radiated at the bit after traveling up the drill string to the bottom-hole assembly/drill pipe interface, where a portion of the energy is reflected and travels back down to the bit. The "drill-string" multiple is radiated at the drill bit after traveling up, and then down the entire length of the drill string. Only a fraction of the multiple energy is radiated at the drill bit. The remainder is reflected back up the drill string and can create secondary rig-generated arrivals, secondary head-wave arrivals, and higher-order multiples.

IDENTIFICATION OF ARRIVALS BASED ON TRAVELTIME AND MOVEOUT

As shown in Rector and Marion (1991), an arrival traveling from the drill bit through the earth to the surface is time-advanced in the drill-bit VSP crosscorrelation function by the traveltime from the drill bit to the top of the drill string. Primary arrivals such as head waves from other locations along the drill string will be time advanced by lesser amounts. For the case of a primary rig-generated arrival, the "correlation time" of the arrival is equivalent to its earth traveltime. In the following sections, we distinguish different drill-bit wave modes based on their correlation time, as well as their moveout with offset and depth.

Identification of arrivals based on offset moveout and correlation time

Figures 7a through 7d show four drill-bit wavefields recorded at the same vertical well where the data in Figure 3 were recorded (Figure 7a is a duplicate of Figure 3). In these displays, the depth of the drill bit increases from 3290 ft (1003 m) in Figure 7a to 7800 ft (2377 m) in Figure 7d. The sediments encountered by the drill bit were clastics ranging in age from late Tertiary to late Cretaceous, resulting in a formation velocity function $V(z)$ that can be reasonably approximated by:

$$V(z) = 5000 \text{ ft/s} + .5z, \tag{5}$$

where z is the depth in feet. In addition to the primary P-wave direct arrival, four other events (a head-wave arrival, a rig-
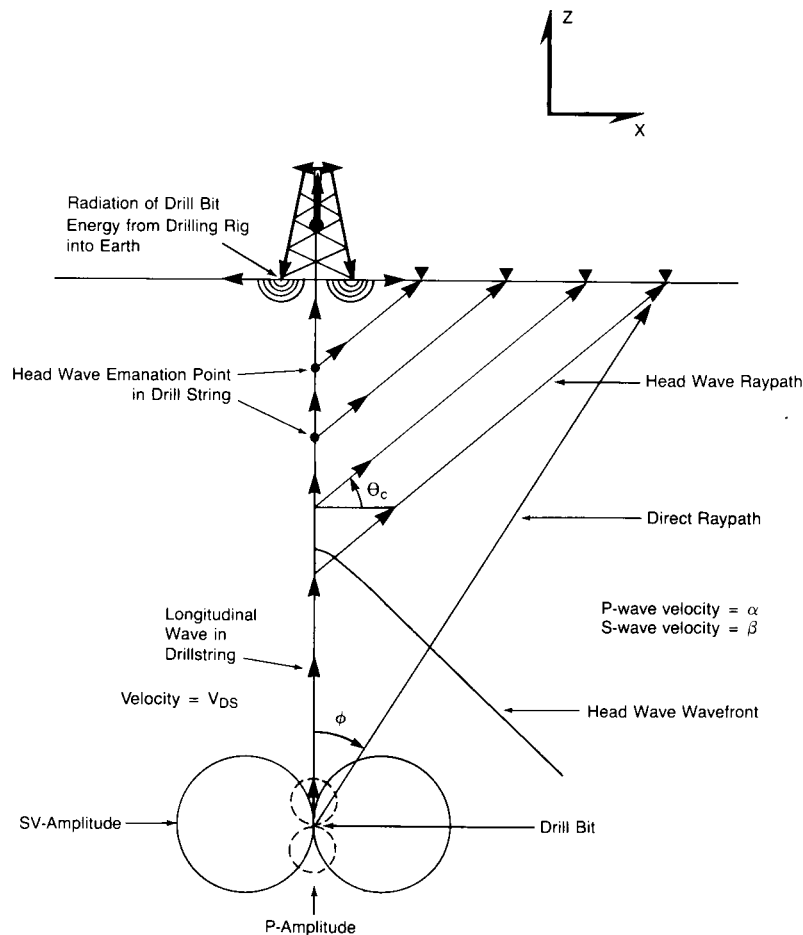

FIG. 6. Drill-bit energy radiated by the drill rig and the drill string. The impacts of the drill-bit teeth at the bottom of the borehole create extensional waves that travel up the drill string and these waves create head waves traveling in the earth provided that the formation velocity, α or β, adjacent to the drill string is less than the drill string velocity V_{DS}. The extensional waves also radiate into the earth through the drill rig and then travel to geophone arrays via near-surface travel paths.

generated arrival, a BHA multiple, and a drill-string multiple) are labeled. Inspection of the wavefields shows that each of these arrivals exhibits a characteristic moveout and arrival time as a function of offset from the wellhead.

The P-wave direct arrival in a vertical well drilling at a depth z exhibits a correlation time t_D that can be approximated by:

$$t_D = \text{traveltime from bit to geophone}$$
$$\text{less traveltime along drill string,}$$

or,

$$t_D = \frac{(x^2 + z^2)^{1/2}}{\alpha} - \frac{z}{V_{DS}}, \tag{6}$$

where α is the average formation P-wave velocity, and a straight raypath between the drill bit and the geophone offset

x is assumed. The moveout of this arrival with offset, $\Delta t_D / \Delta x$, is then:

$$\frac{\Delta t_D}{\Delta x} = \frac{\sin \phi}{\alpha}, \tag{7}$$

where ϕ is the take-off angle of the direct arrival with respect to the vertical. This moveout is equivalent to the moveout with offset that would be observed in a walkaway VSP. The delay and moveout of the direct arrival in Figures 7a through 7d correspond closely with the traveltimes and moveouts computed using the velocity function.

The BHA and drill-string multiples arrive later than the P-wave direct arrival with correlation times t_{BHA} and t_{DS} given by:
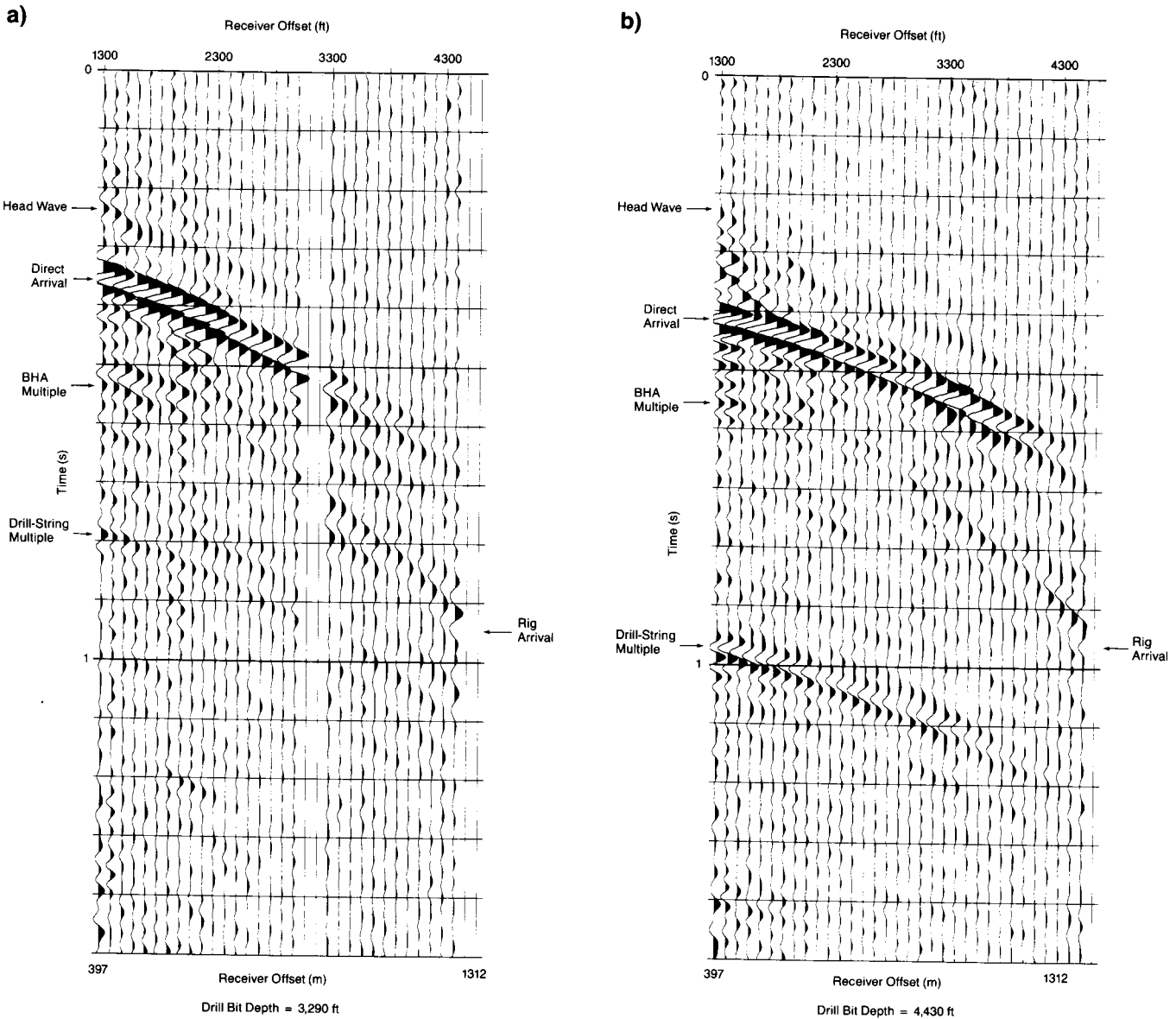

FIG. 7. (a) Vertical geophone data recorded when the drill bit was drilling at depths of 3290 ft (1003 m), (b) 4430 ft (1350 m), (c) 5610 ft (1710 m), and (d) 7800 ft (2377 m) in a vertical well.

$$t_{BHA} = t_D + \frac{2L_{BHA}}{V_{DS}} ,$$ (8)

and

$$t_{DS} = t_D + \frac{2z}{V_{DS}} ,$$ (9)

where L_{BHA} is the length of the BHA. The drill string and BHA multiples have the same moveout with offset as the P-wave direct arrival.

Unlike the hyperbolic moveout with offset of the direct and drill-string multiple arrivals, the rig arrivals in Figures 7a through 7d exhibit nearly linear moveout with receiver offset. At this well location, these arrivals travel with a phase velocity between 4500 and 6000 ft/s (1372 and 1830 m/s), and a group velocity of about 4800 ft/s (1463 m/s). The most

likely travel path for these arrivals is a near-surface P refraction or a wide-angle P reflection off a near surface layer. The group and phase velocities are similar to the group and phase velocities observed in the "first breaks" from conventional surface seismic shot records in the region.

Like the rig arrivals, the head-wave arrivals labeled in Figures 7a through 7d exhibit nearly linear moveout with wellhead offset. They can be distinguished from the rig arrivals based on their correlation time. At an offset of 2300 ft (700 m), the head-wave correlation time is more than 100 ms earlier than the rig arrival. Since no arrival from the drill rig can occur before the first break time, this arrival comes from an apparent source position along the drill string. The head-wave correlation time is advanced from its traveltime through the earth by z_H/V_{DS}, where z_H is the distance from the head-wave radiation depth along the drill string to the pilot sensor at the top of the drill string.

c)

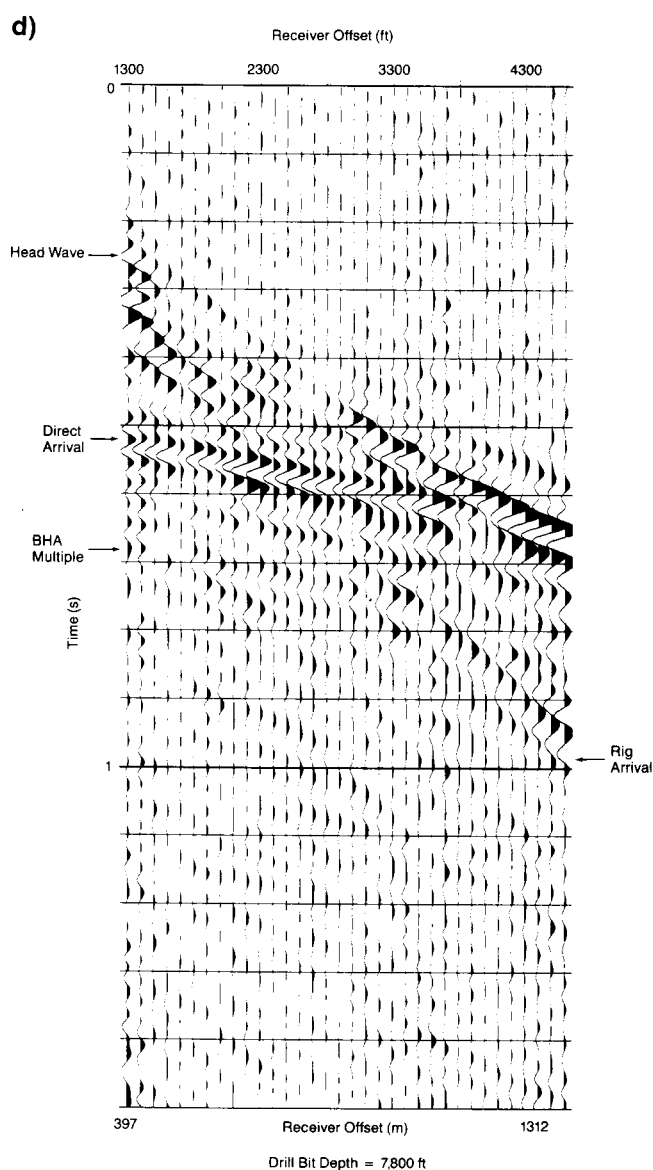Drill Bit Depth = 5,610 ft
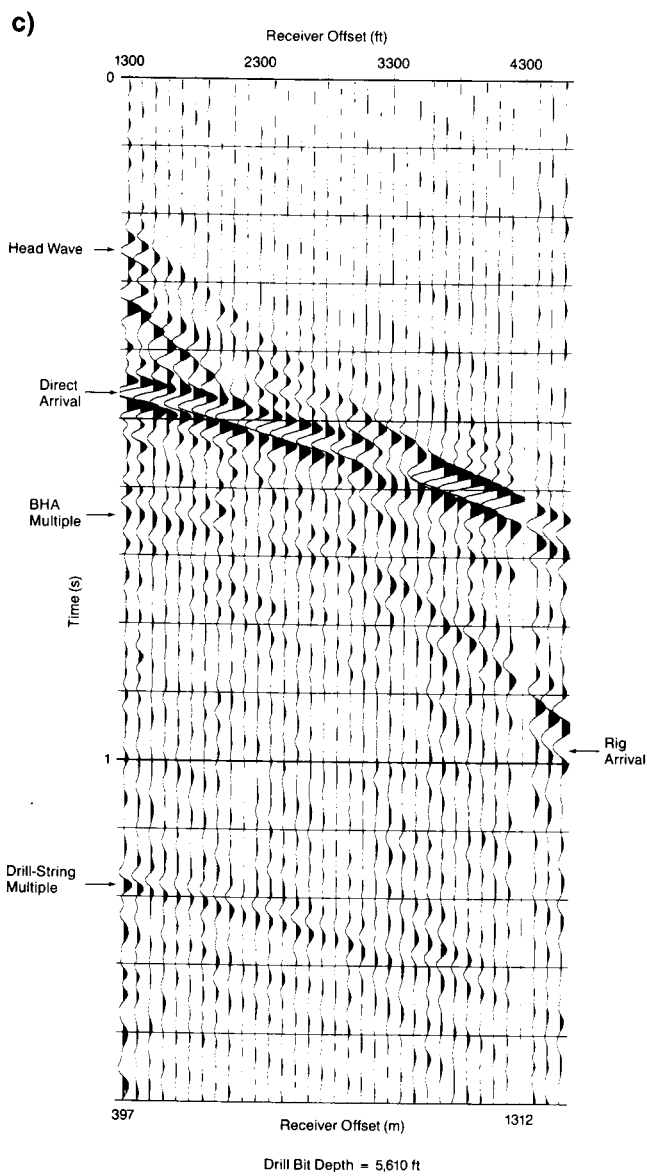
d)

Drill Bit Depth = 7,800 ft

FIG. 7. Continued.

The head-wave arrival can be distinguished from *point* sources along the drill string based on moveout with offset. If these arrivals were point sources along the drill string, they would exhibit hyperbolic moveout like the direct arrival.

Assuming a homogeneous earth, the head-wave apparent velocity with offset, $\Delta x/\Delta t_H$, is:

$$\frac{\Delta x}{\Delta t_H} = \frac{\alpha}{\cos \theta_c}. \tag{10}$$

This expression can be obtained from Dobrin's (1960) expressions for head-wave moveouts. The apparent velocity is independent of the source depth and is only dependent upon the formation velocity adjacent to the drill string and the inclination of the drill string.

Figure 8 shows the occurrence of head waves on a vertical well drilled in a constant velocity earth as a function of offset, depth, and formation velocity at depth. Given a velocity function that increases with depth, the receiver offset will be somewhat less than those depicted in Figure 8, and an individual offset can record several head-wave arrivals from different source depths. Near offsets receive head waves from drill-string depths corresponding to shallow, low velocity formations and deep, high velocity formations. Longer receiver offsets record head waves over a wider range of drill-string depths for lower velocity formations, but

they do not receive head waves for very high formation velocities at most drill string depths of interest.

The offset-moveout differences between the head-wave/rig arrivals and the direct arrivals from the bit can be used to separate the arrivals by beamforming a group of receivers. Alternatively, as shown in Figure 8, it may be possible with a knowledge of $v(z)$ to place the receivers so as to avoid recording large P head waves. For example, a 10 000 ft (3048 m) well drilled in constant 15 000 ft/s (4572 m/s) rock produces P head waves that can be recorded only to an offset of around 3000 ft (914 m). Past this position the arrival is a wearer diffraction.

Identification and separation of arrivals based on moveout with depth

Figure 9 shows a series of correlated drill-bit wavefields from a geophone array located 2532 ft (772 m) from the wellhead. The data were recorded on a vertical well drilled in sediments similar to the well where the data in Figures 7a through 7d were acquired. The linear geophone array used to record upcoming P-waves consisted of forty-eight 10 Hz geophones oriented toward the wellhead with a total aperture of 300 ft (91 m). This array attenuated the head-wave and rig arrivals observed in Figures 7a through 7d while preserving the longer wavelength P-wave direct arrivals at
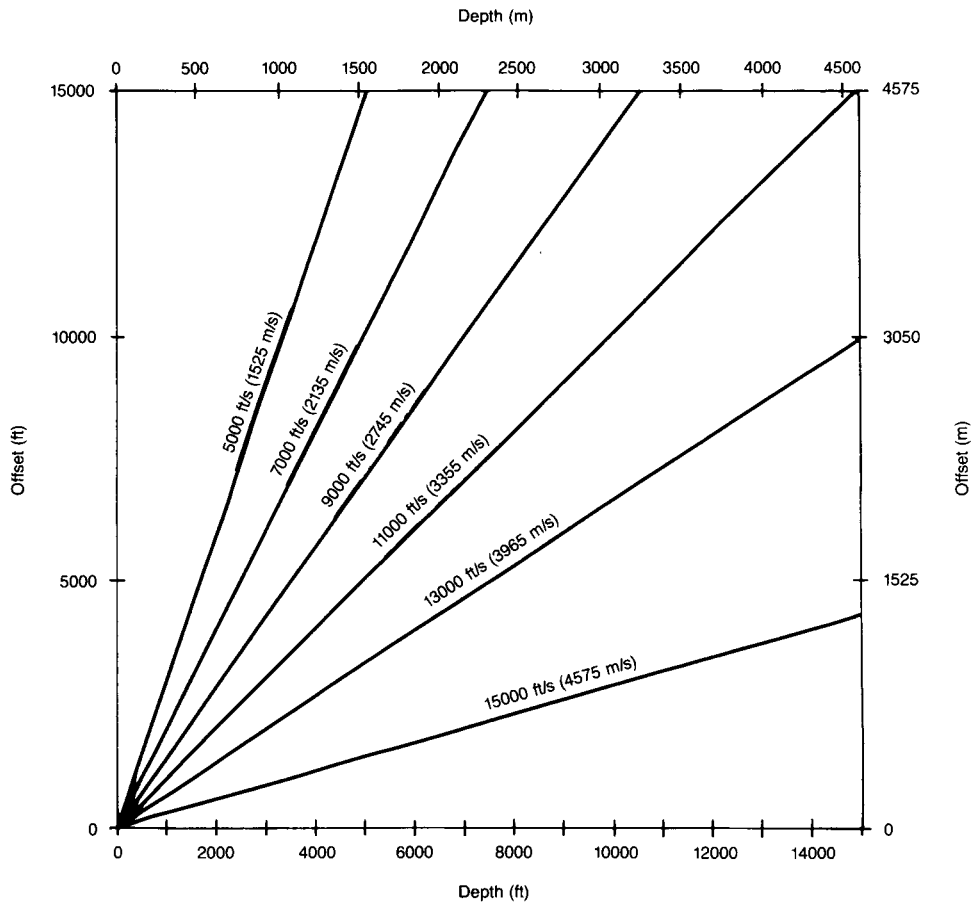

FIG. 8. Head-wave arrival intersection with the drill string and with the surface as a function of formation velocity. A vertical borehole and a homogeneous earth have been assumed.

most depths. The arrivals identified in Figures 7a through 7d are also labeled in Figure 9, as well as an event reflected from below the drill bit. Each of the arrivals has a characteristic moveout as a function of drill-bit depth.

Assuming a straight raypath between the drill bit and the surface receiver, the moveout with depth of the drill-bit direct arrival in a vertical borehole is:

$$\frac{\Delta t_d}{\Delta z} = \frac{\cos\phi}{\alpha} - \frac{1}{V_{DS}}, \tag{11}$$

This expression can be obtained by differentiating equation (6).

Likewise, the moveout of a reflection from a horizontal interface just beneath the drill bit is approximately given by:

$$\frac{\Delta t_r}{\Delta z} \sim -\frac{\cos\phi}{\alpha} - \frac{1}{V_{DS}} \tag{12}$$

The corresponding moveout equations for a conventional VSP omit the term $1/V_{DS}$. Therefore, the moveout of the correlated P-wave direct arrival over depth is always less than the moveout of an equivalent VSP direct arrival, and the negative moveout of the reflection arrivals is always greater than the corresponding negative moveout of equivalent VSP reflection arrivals. Moreover, the direct arrival can exhibit zero, or even negative moveout with depth (if ϕ or α becomes large); whereas, an arrival from a reflection below the drill bit always exhibits negative moveout. In Figure 9, the direct arrival exhibits positive moveout and the drill-bit reflections exhibit negative moveouts. This is consistent with the expected formation P-wave velocities in the vicinity of the borehole (which are similar to those depicted in Figures 7a through 7d).

The BHA multiple arrival in Figure 9 exhibits a moveout with depth that mimics the P-wave direct-arrival moveout
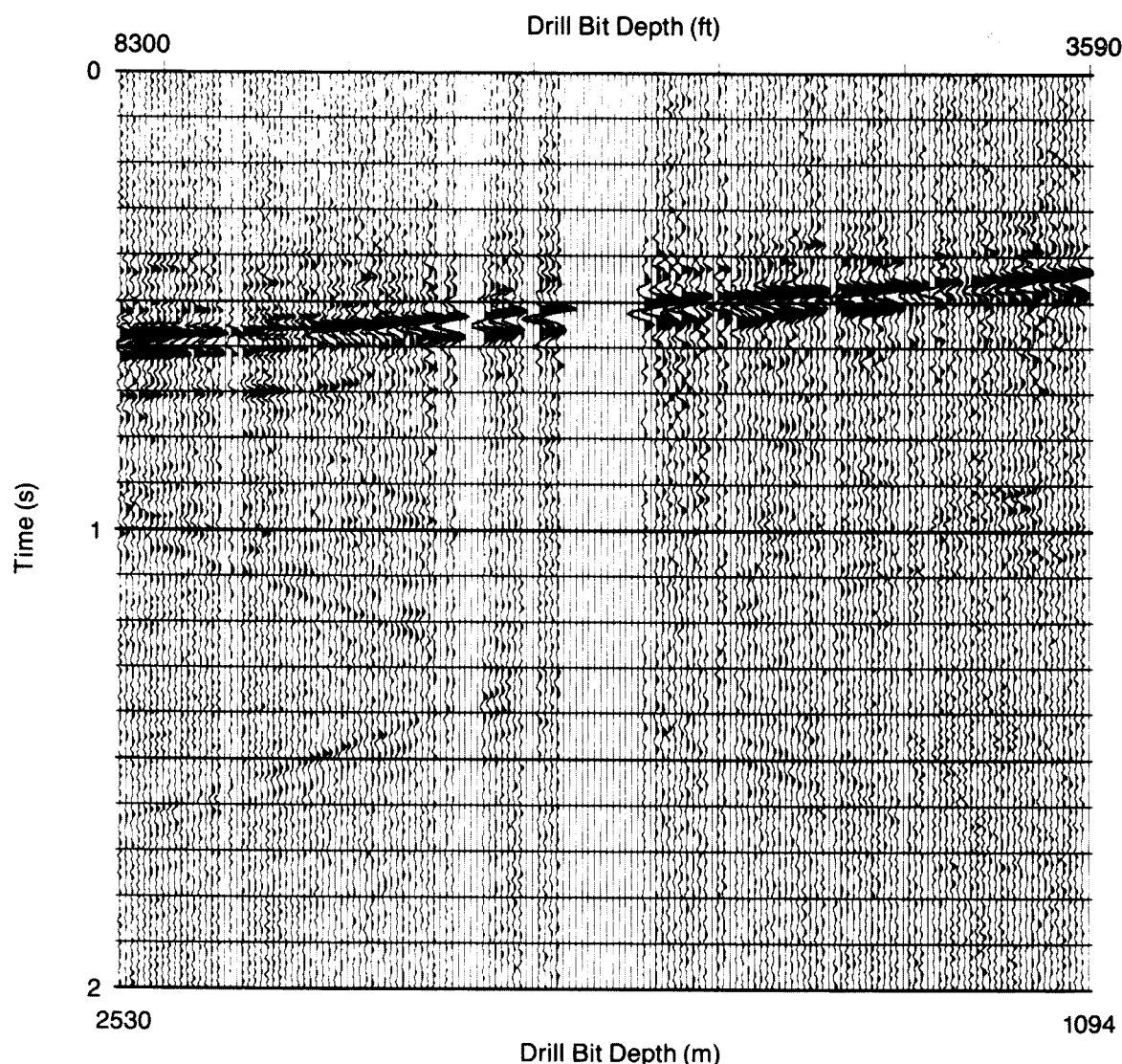

Fig. 9. Drill-bit wavefields from a geophone group located 2532 ft (772 m) from the wellhead. The traces represent wavefields generated at 30 ft (9.1 m) intervals as a roller-cone bit drilled from 3590 to 8300 ft (1094 to 2530 m).

since the BHA multiple occurs at a constant time lag relative to the direct arrival given by equation (8). In Figure 9, the BHA length was approximately 800 ft (244 m), which resulted in t_{BHA} = 100 ms. Like earth-path multiple arrivals in conventional VSP, the BHA multiples can be attenuated through deconvolution of the direct arrival.

In Figure 9, the drill-string multiple arrival exhibits a moveout that is approximately double that of the direct arrival. Referring to equation (9), the moveout with depth of the drill string multiple relative to the direct-arrival moveout, $\Delta t_{DS}/\Delta z$, is:

$$\frac{\Delta t_{DS}}{\Delta z} = \frac{2}{V_{DS}}.$$ (13)

In Figure 9, the head-wave arrival time exhibits no change as the depth of the drill bit increases. Since the intersection of the head wave with the drill string is the same regardless of the depth of the drill bit, its drill string-to-receiver path does not change with drilling depth. Thus the head-wave arrival exhibits zero moveout as a function of drilling depth in a series of crosscorrelation functions. Another way to describe this phenomenon is that the head wave traveling in the earth is created by the extensional wave traveling up the drill string, which is the same wave that the pilot signal records. As the drill bit moves deeper, both the head-wave arrival recorded by the geophone array and the extensional-wave arrival recorded by the pilot sensor are delayed by the same factor, and therefore the moveout of the head-wave arrival is zero regardless of the receiver offset, the borehole deviation, or the formation velocity. The depth at which the head wave intersects the direct arrival determines the intersection depth of the head wave and the drill string. The head wave does not exist above this intersection depth, resulting in a step function behavior over depth. In Figure 9, the head waves recorded at this receiver location intersected the drill string slightly above 3000 ft (914 m).

Rig-generated arrivals also have zero moveout with depth. The extensional wave that the pilot sensor records most likely propagates into the earth after traveling past the pilot sensor, up the drilling lines, and into the rig mast. Therefore, correlation time does not change as the length of the drill string increases. Unlike the step-function behavior of the head-wave arrival, the rig arrival is continuous over depth. The moveout differences between the different arrivals in Figure 9 suggest that conventional VSP wavefield separation techniques can be used to extract the primary drill-bit direct and reflected arrivals. Since the rig and head-wave arrivals have zero moveout with depth, a filter that rejects events that appear to move along the depth axis with infinite apparent velocity (zero spatial frequency) will attenuate these events.

To remove the rig and head-wave arrivals in Figure 9, a median filter was chosen because of its ability to pass step functions (Hardage, 1985) like the head-wave arrival. Figure 10 shows the residual resulting after (1) enhancing the data in Figure 9 with a 55 trace median filter and (2) subtracting the enhanced data from the original data in Figure 9. The distance spanned by 55 traces (1680 ft, 512 m) was the average apparent wavelength of the direct arrival at the low end of the frequency spectrum (13 Hz). The zero-moveout interference is substantially attenuated in Figure 10. Only primary direct and reflected drill-bit arrivals and drill-string multiples are evident.

CONCLUSIONS

The following wave phenomena occur when drill-bit teeth impact at the bottom of a borehole:

1) P, SV, and SH body waves are generated at the point of impact. In the far-field, the P-wave amplitudes are largest along the borehole axis and progressively weaken away from the axis until no P-waves are radiated perpendicular to the borehole. The SV and SH waves have radiation patterns rotated 90 degrees from the P-wave radiation pattern. At an angle of 45 degrees from the borehole axis, the SV displacement amplitude is larger than the P-wave amplitude by a factor of (α^2/β^2). The SH displacement amplitude is about three orders of magnitude less than the SV displacement amplitude. The radiation patterns have symmetry of rotation about the borehole axis.

2) Rig-generated arrivals originate at the drill bit, travel up the drill string into the rig mast, and then into the earth where they travel via predominantly near-surface paths to surface receivers.

3) Head-wave arrivals are present when the formation velocity adjacent to the drill string is less than the longitudinal wave velocity in the drill string. These head waves propagate as a conical wavefront in the earth, with a wavefront angle with respect to the borehole axis defined by equation (4). The head-wave wavefronts are nearly parallel with the borehole axis when the formation velocity is very low, and are nearly perpendicular to the borehole axis when the formation velocity approaches the drill string velocity.

4) Multiple body wave arrivals are radiated at the drill bit when the longitudinal wave traveling in the drill string undergoes one or more reflections at drill string discontinuities.

These arrivals have characteristic traveltimes and moveouts in drill-bit crosscorrelation functions that are dependent upon the formation velocities near the borehole, the receiver offset from the drill bit, and in some cases, the depth of the drill bit. The differences in the spatial characteristics of these arrivals in a time-versus offset or a time-versus depth display provide a means by which individual wave modes can be identified and separated using spatial filtering techniques.

The drill-bit radiation pattern is particularly well suited for applications such as P-wave velocity surveys and P-wave zero offset imaging in vertical boreholes. Deviated borehole P-wave velocity surveys and reflection imaging around the borehole can be accomplished, provided that some of the surface receivers are deployed to avoid the P-wave radiation null zone. In a vertical well, SV-wave velocity surveys and shear/converted wave images are obtainable if the receiver is offset from the borehole. SV-wave surveys on a vertical well drilled in a horizontally layered earth will produce low-level signals at very near receiver offsets.
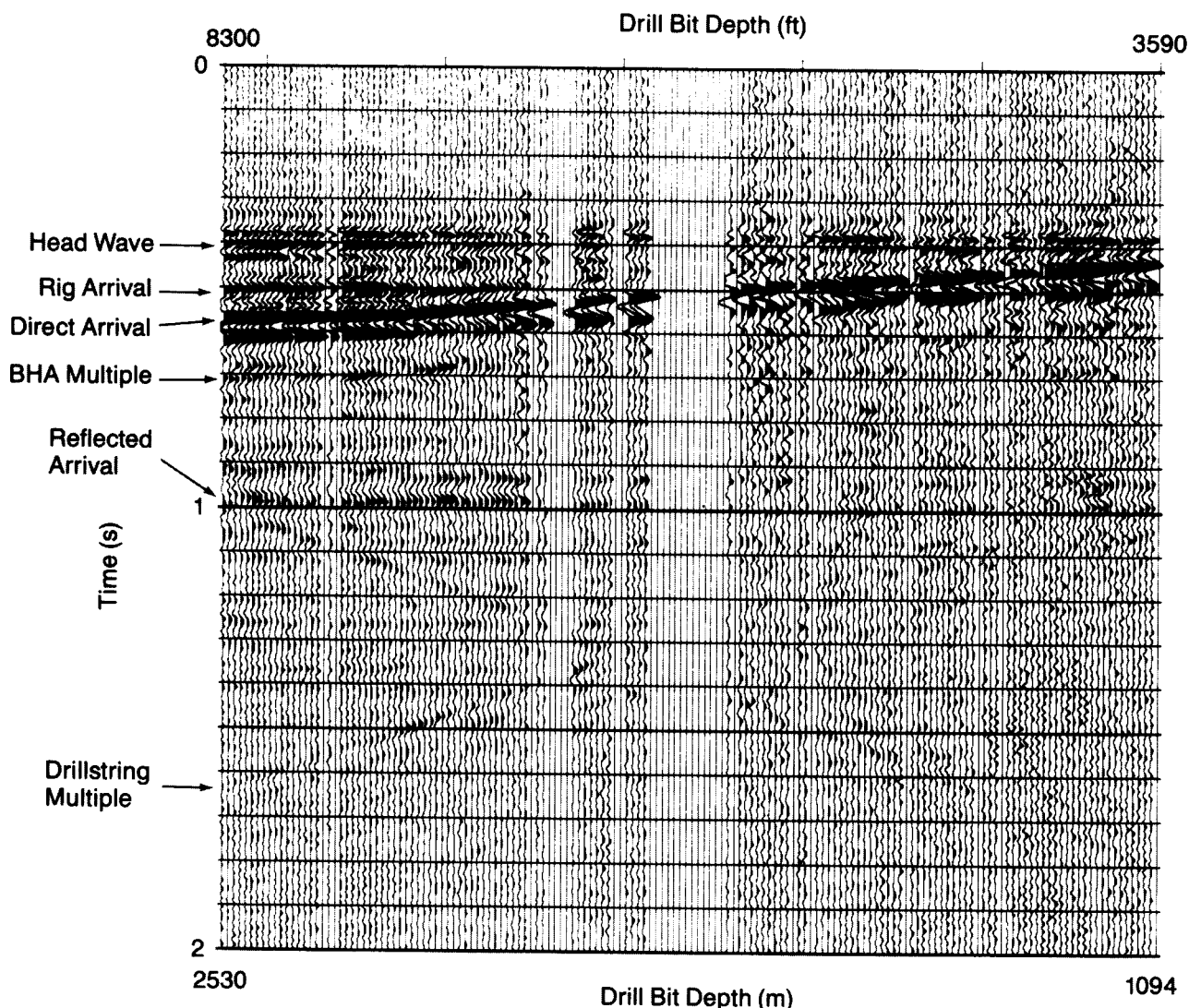
FIG. 10. Residual after subtracting the 55 trace enhanced wavefield from the wavefield in Figure 9.

In a horizontal well, SV waves will be recorded vertically above the drill bit which opens up a large area of investigative possibilities. However, vertically-incident P-wave surveys will be lower amplitude given the drill-bit radiation pattern in horizontal wells.

For cross-borehole applications between vertical wells, drill-bit impacts are also a good source of SV-wave energy but a low-level source of P-wave energy.

REFERENCES

Adams, N. J., 1986, Drilling engineering: A complete well planning approach: PennWell Publ. Co.
Dobrin, M. B., 1960, Introduction to geophysical prospecting: McGraw-Hill Book Co.
Hardage, B. A., 1985, Vertical seismic profiling, Part A: Principles: Pergamon Press Inc.

Heelan, P. A., 1953, Radiation from a cylindrical source of finite length: Geophysics, 18, 685–696.
Meredith, J., 1990, Numerical and analytical modeling of downhole seismic sources: The near and far field: Ph.D. thesis, Massachusetts Institute of Technology.
Rector, J. W., and Marion, B. P., 1991, The use of drill-bit energy as a downhole seismic source: Geophysics, 56, 628–634.
Samec, P., and Kostov, C., 1988, Full waveform modeling of a downhole source radiation pattern using a finite-element technique: 58th Ann. Internat. Mtg., Soc. Expl. Geophys., Expanded Abstracts, 143–145.
Sheppard, M. C., and Lesage, M., 1988, The forces at the teeth of a drilling roller-cone bit—theory and experiment: SPE Paper 18042, 63rd Ann. Tech. Conf., Soc. Petr. Eng. of AIME.
Squire, W. D., and Whitehouse, H. J., 1979, A new approach to drill-string acoustic telemetry: 54th Ann. Tech. Conf., Soc. Petr. Eng. of AIME.
Vennin, H. C., 1989, Drilling bit optimized for the Paris Basin: Oil and Gas J., no. 7, 93–96.
White, J. E., 1965, Seismic waves: Radiation, transmission, and attenuation: McGraw-Hill Book Co.

APPENDIX
MATHEMATICAL DESCRIPTION OF FAR-FIELD DRILL STRING WAVE BEHAVIOR

The general solution for axially-symmetric wave propagation around a vertical borehole in cylindrical coordinates is (White, 1965):

$$\Phi = [A_1 H_0^{(1)}(mx) + A_2 H_0^{(2)}(mx)]e^{-i\ell z}e^{i\omega t},$$

$$\Theta = [B_1 H_1^{(1)}(kx) + B_2 H_1^{(2)}(kx)]e^{-i\ell z}e^{i\omega t},$$

$$1 = \frac{\omega}{c}, \quad m = \omega\left(\frac{1}{\alpha^2} - \frac{1}{c^2}\right)^{1/2}, \quad k = \omega\left(\frac{1}{\beta^2} - \frac{1}{c^2}\right)^{1/2}, \quad (A-1)$$

where α is the compressional velocity of the formation, β is the shear velocity of the formation, c is the propagation velocity in the borehole (which will be defined as the longitudinal wave velocity up the drill string), x is the perpendicular distance from the borehole axis, ω is angular frequency, $H_0^{(1)}$, $H_0^{(2)}$, $H_1^{(1)}$, $H_1^{(2)}$ are modified Hankel functions as described by White (1965), and Φ and Θ are scalar potentials satisfying the wave equation in cylindrical coordinates. The arguments of the Hankel functions H_0 and H_1 in equation (A-1) will be real, provided that $\beta < c$ and $\alpha < c$. If $\beta < c$ and $\alpha > c$, then the argument of H_1 will be real and the argument of H_0 will be imaginary. If both α and β are greater than c, then both arguments are imaginary. When an extensional wave propagates up a steel drill string, both arguments are generally real for most sedimentary sections.

White noted that Hankel functions of large, real arguments can be approximated as:

$$H_0(mx) \sim \left(\frac{2}{\pi mx}\right)^{1/2} e^{\pm i(mx - \pi/4)},$$

$$H_1(kx) \sim \left(\frac{2}{\pi kx}\right)^{1/2} e^{\pm i(kx - 3\pi/4)}, \quad (A-2)$$

and Hankel functions of large, imaginary arguments take the form:

$$H_0(imx) \sim A_1 e^{-mx},$$

$$H_1(ikx) \sim B_1 e^{-kx},$$

where,

$$m = |\omega|\left(\frac{1}{c^2} - \frac{1}{\alpha^2}\right)^{1/2}, \quad k = |\omega|\left(\frac{1}{c^2} - \frac{1}{\beta^2}\right)^{1/2}. \quad (A-3)$$

Using these approximations, the far-field solution for wave behavior around a cylindrical borehole can be split into two conditions that depend upon whether the arguments are real or imaginary (i.e., upon the compressional and shear velocities, α and β, of the formation surrounding the borehole and the velocity of propagation in the borehole c).

Condition 1: $\beta < \alpha < c$.

If both the compressional and shear velocities are less than the propagation velocity up the drill string, then in the far-field, the potentials Φ and Θ for waves traveling in the $+z$ direction (upwards) become:

$$\Phi \sim \frac{1}{(xm)^{1/2}} e^{-imx}e^{-i\ell z}e^{i\omega t}$$

$$\Theta \sim \frac{1}{(xk)^{1/2}} e^{-ikx}e^{-i\ell z}e^{i\omega t}. \quad (A-4)$$

These potentials define head waves that propagate away from the borehole as plane waves making an angle θ_c, with respect to the perpendicular to the borehole axis. For the compressional potential Φ,

$$\theta_c = \sin^{-1}\left(\frac{\alpha(Z)}{c}\right), \quad (A-5)$$

and for the shear potential Θ,

$$\varphi_c = \sin^{-1}\left(\frac{\beta(Z)}{c}\right). \quad (A-6)$$

The compressional potential Φ, defines a head wave that propagates into the earth at the compressional velocity, whereas the shear potential Θ, defines a head wave that propagates at the shear velocity.

As equation (A-4) shows, the head-wave amplitude decreases as $1/(x)^{1/2}$ away from the borehole. Equation (A-4) also shows that the head-wave amplitude increases as α and β approach c, the velocity of propagation in the drill string. In the near-field, the Hankel functions approach a constant value, and the expressions in Equation A-1 become:

$$\Phi \sim e^{-i\ell z}e^{i\omega t},$$

$$\Theta \sim e^{-i\ell z}e^{i\omega t}. \quad (A-7)$$

Both of these potentials define a displacement in the z-direction, which travels with a velocity c, and as depicted in Figure 8, the wavefront bends toward the normal to the borehole axis as radial decreases.

Condition 2: $\beta < c < \alpha$.

If the compressional velocity is greater than the velocity of the longitudinal wave traveling up the drill string, then the argument of the zero-order Hankel functions H_0 in equation (A-3) is imaginary, and the compressional potential in the far-field becomes:

$$\Phi \sim H_1 e^{-mx}e^{-i\ell z}e^{i\omega t},$$

where

$$m = |\omega|(1/c^2 - 1/\alpha^2)^{1/2}. \quad (A-8)$$

This form defines a guided wave traveling up the borehole with a velocity equal to the longitudinal wave velocity in the drill string. Due to its exponential decay away from the borehole wall, this wave does not propagate appreciably into the earth. The shear potential Θ, is the same as in equation A-4, and shear head waves are radiated into the earth as before.